Full Text View

Volume 29, Issue 6 (June 1999)

Journal of Physical Oceanography
Article: pp. 1180–1207 | Abstract | PDF (645K)

Loop Current Eddy Paths in the Western Gulf of Mexico

Peter Hamilton

Science Applications International Corporation, Raleigh, North Carolina

G. S. Fargion*

Department of Marine Biology, Texas A&M University, Galveston, Texas

D. C. Biggs

Department of Oceanography, Texas A&M University, College Station, Texas

(Manuscript received March 19, 1997, in final form June 25, 1998)

DOI: 10.1175/1520-0485(1999)029<1180:LCEPIT>2.0.CO;2

ABSTRACT

The paths of anticyclonic Loop Current eddies in the western Gulf of Mexico have been investigated using ARGOS-tracked drifters accompanied by hydrographic surveys. The analysis used orbit parameters derived from a least square fit of a translating ellipse kinematic model and showed that paths from four quite different eddies had a number of similar features. They are a general increase in rotational period over time, clockwise rotation of ellipse axes that slows with time and often becomes stationary in the far western Gulf, swirl velocities that decay quite slowly, and a tendency of the eddies to have low divergence. In three cases, 20- to 30-day oscillations of the orbit parameters were observed. Translation velocities of the orbits showed the characteristic stalls and sprints that have been previously observed. In two cases, stalls and deviations from solid body rotation could be attributed to the presence of vigorous lower continental slope cyclones situated to the northwest of the eddies in question. Comparison of relative vorticity, calculated from orbits and hydrography, showed reasonable agreement though deviations from solid body rotation were found in all cases. Vorticity also remained fairly constant for the 3–6-month periods investigated. Major perturbations were tentatively attributed to absorption of weaker, older Loop Current anticyclones in the western Gulf.

Statistics on eddy characteristics, derived from drifters, were compiled for 10 eddies between 1985 and 1995. The paths were separated into two, east and west of 94°W, corresponding to the deep western basin and under the influence

- D. C. Biggs

of the steep western slope, respectively. The paths occupied a broad band of 2°–3° latitude in width in the center of the basin with a mean west-southwest trend. There were no apparent preferred paths either in the main basin or near the western slope where eddies were equally likely to move northward or southward along the boundary. Eddy paths also showed frequent occurrences of 20- to 30-day anticyclonic perturbations similar to that found from the individual analyses.

1. Introduction

The characteristics of large Loop Current (LC) anticyclonic eddies have been derived primarily from numerous satellite-tracked drifters over the past decade and a half. Kirwan et al. (1984b) introduced a model of a translating ellipse for kinematic analysis of drifter paths in eddies, and it has been applied to LC eddies in the western Gulf of Mexico. A similar model for eddy drifter paths, but using a more straightforward least square fit approach to derive the ellipse parameters, was developed by Glenn et al. (1990). This latter model has been adopted for this study. Kinematic analyses have been used for eddies approaching the western Mexican slope in the southwest around 23°N (Kirwan et al. 1984b, 1988) and around 25°N (Lewis et al. 1989). The latter, known as “Fast Eddy” or eddy B, was modeled numerically by Smith (1986), and many features of the interaction with the slope were captured. They include the distortion of the nearly circular eddy as it approached the slope, the generation of a companion cyclone to the north, and the subsequent movement of the anticyclone–cyclone pair eastward, off the slope, and southward. Glenn and Ebbesmyer (1993) tracked a major western gulf eddy with multiple buoys. They showed that, once free of the LC, its path across the Gulf was characterized by alternate sprints and stalls. During the sprints, the eddy was essentially in solid body rotation. However, in the stalls the effects of topographic and planetary Rossby wave dispersion were evident in the displacements of the centers of different simultaneous orbits such that centers of the buoys with increasing radii were displaced in the direction of propagation realized in the subsequent sprint. The reasons for the stalls were not determined, but there were some hints from other data that other features may have played a role.

As anticyclones approach the steep Mexican slope in the western Gulf, there are complex interactions with the existing eddy field, including remnants of older LC anticyclones and the slope topography. Vidal et al. (1994) documented a case, from an extensive hydrographic survey of a large portion of the western Gulf where the anticyclone was sandwiched between two cyclones. The cyclones were large and vigorous and were apparently gaining mass and vorticity from the anticyclone. Strong onshore–offshore transports occurred between the eddies, affecting exchange with the narrow Mexican shelf. Similar kinds of complexity, usually involving cyclone–anticyclone pairs, have been shown to exist along the western boundary by Merrell and Morrison (1981), Brooks and Legeckis (1982), and Vidal et al. (1992). Biggs et al. (1996) described the interaction of eddy Triton with a vigorous cyclone in the western Gulf that resulted in the anticyclone being split into two parts. The existence of persistent cyclones in the central basin and over the northern Louisiana–Texas slope, which were apparently not directly connected to LC eddies, was shown by Hamilton (1992).

Kinematic analyses of drifters, and most theoretical models (e.g., Smith 1986; Nof 1988), tend to treat LC eddies as isolated features. There is increasing evidence from hydrographic surveys (e.g., Vidal et al. 1994), and more recently satellite altimetry (Johnson et al. 1992; Leben et al. 1993), that the eddies are propagating through a field of features, and this helps to explain the variety of paths and translation velocities of these eddies in the central and western Gulf. Despite this, the orbital periods, velocities, and relative vorticities of eddies not interacting with the western boundary or merging with another anticyclone remain reasonably consistent with being in an isolated feature. This implies that most of the exchange of mass, momentum, and vorticity occurs at the periphery and does not strongly affect the central core where drifters typically orbit.

The present study extends the case histories of LC eddies using drifters deployed during the LATEX[1] program. Eddies U, V, W, and Y were seeded with drifters. Prior to this sequence, eddy T separated from the LC in June 1991 and has been analyzed by Biggs et al. (1996). A difference with previous drifter-based analyses is that these eddies were surveyed by ship and aircraft a number of times, particularly when they were close to the northern slope. Properties derived from hydrographic surveys (including a few AXCP profiles) can be compared to those derived from the drifters. Events captured by both drifters and hydrographic surveys that provide information on the interactions of LC anticyclones with other eddies are a major focus of this paper.

Previous analysis of the statistics of eddy paths in the western Gulf was performed by Vukovich and Crissman (1986) using satellite Advanced Very High Resolution Radiometer (AVHRR) imagery. They found three preferred paths, the most common being the southwesterly path implied by planetary and topographic Rossby wave dispersion; the least common, a path parallel to the northern slope such as that taken by eddy B (Lewis et al. 1989). This database of AVHRR imagery was limited to the winter months with the usual problems of tracking eddies from AVHRR imagery when extensive cloud cover is often present. In this study, the ensemble statistics of 10 eddies that were tracked using drifters between 1985 and 1995 have been compiled and analyzed.

2. Data

The database consists primarily of drifter tracks and hydrographic surveys using aircraft-deployed AXBTs and AXCPs and ship-deployed XBTs and CTD casts. Current meter data is available from the shelf break moorings deployed by the LATEX A program. Tables 1 and 2 give the details on the ARGOS-tracked drifters and hydrographic surveys, respectively. All the drifters are clearwater World Ocean Circulation Experiment (WOCE)–type drifters with holey sock drogue elements with the indicated dimensions (Table 1). Between three and eight ARGOS position fixes per day are usual for a drifter in the Gulf of Mexico. The AXBT/AXCP flights were conducted by the LATEX C program and the slope hydrographic cruises by the Texas A&M University Gulf Cetacean surveys (GulfCet) and Ship of Opportunity Program (SOOP) projects. CTD stations were sampled with a Sea Bird 9/11 and were taken at approximately 75-km intervals. XBTs were used between CTD stations to increase the resolution of the sampling. The LATEX A program deployed conventional taut-line moorings on the 200-m isobath on the Texas shelf. Each mooring was equipped with three current m, an Endeco at 10 or 12 m, and two Aanderaa RCM4s at 100 m and 10 m from the bottom. The positions are given in Fig. 1. Moorings 49 and 12 were deployed in water depths of 500 m. These data were used to enhance the velocities obtained from the aircraft surveys as appropriate.

a. Buoy orbit analysis

The drifter position data are filtered and smoothed using a modification of the method of successive corrections and Gaussian filters given by Pedder (1993). The modification calculates smoothed and interpolated latitudes and longitudes of the positions as a function of time rather than a constructed gridded field in two-dimensional space as in the original method. The influence timescale for the drifter tracks is usually 28 h. Thus, motions with timescales less than about 3 days are filtered out of the smoothed drifter tracks. The positions age resampled at 6-h intervals. Smoothed and filtered tracks are used for all calculations and figures (e.g., Fig. 1).

The drifter tracks are analyzed by least square fitting a diverging, translating ellipse to the smoothed position data. The method follows Glenn et al. (1990). The equations fit to a drifter orbit are

$$x(t) = x_0 + ut + (1 + Dt) \times [a\cos\theta\cos(-\omega t + \phi) - b\sin\theta\sin(-\omega t + \phi)] \quad (1)$$

$$y(t) = y_0 + vt + (1 + Dt) \times [a\sin\theta\cos(-\omega t + \phi) + b\cos\theta\sin(-\omega t + \phi)], \quad (2)$$

where

1. x, y are the coordinates of the modeled buoy track;
2. x_0, y_0 is the $t = 0$ center position of the ellipse;
3. u, v are the x and y components of the center translation velocity;
4. a, b are the major and minor axes of the ellipses;
5. θ is the inclination of the major axis to the east or x axis;
6. ω is the orbital frequency;
7. ϕ is the $t = 0$ phase of the orbit;
8. D is the divergence.

Latitudes and longitudes are transformed into the (x, y) coordinate system using standard f-plane projections. Minor differences from the Glenn et al. (1990) method of least square fitting (1) and (2) to buoy positions are that the smoothed equally spaced tracks are used, (u, v) are constrained to be (dx_0/dt, dy_0/dt), and that the period T, over which the orbit is fit, adapts by iteration so that $T^{(k)} = 2\pi/\omega^{(k-1)}$, where $\omega^{(k)}$ is given by the least square solution to (1) and (2). Thus, all that is required is an estimate of $T^{(0)}$ for the first orbit of the drifter track. Here T is allowed to change by daily increments between sets of iterations until convergence.

The estimation of the parameters proceed by daily increments with the results of the previous least square fit providing the initial estimates for the current calculation. The adaption of T to the calculated orbit frequency was found to improve the χ^2 of the fit in almost all cases over assuming a constant period for the orbit fits. Thus, it is not necessary to segment a drifter track into sections where different orbit periods (found by trial and error) predominate as in Glenn et al. (1990). The model fits work satisfactorily when there are data points in all four quadrants of the elliptical orbit. The advantages of using Glenn et al. (1990) over the original method of Kirwan et al. (1984b; 1987) are primarily the advantages accruing from robust nonlinear least square methods. Both methods essentially solve the same kinematic equations; therefore, there should be no significant differences in results from either model.

Useful quantities derived from the ellipse parameters include the geometric mean radius $r\omega = (ab)^{1/2}$, the mean swirl velocity r, the ellipse eccentricity $e = a/b$, and the relative vorticity ζ, where

$$\zeta = -\omega(e + 1/e). \quad (3)$$

This latter formula assumes that the eddy is in solid body rotation and, for a circular eddy, depends only on the period of rotation.

b. AXCP profiles

The velocity shear profiles from the AXCPs are smoothed by least square fitting cubic splines to the u and v components. This removes most of the high-frequency fluctuations with wave numbers greater than ~ 20 to 50 m^{-1}. There is considerable inertial–internal wave energy in most of these profiles. The XCP measures velocity relative to a reference velocity that is constant with depth. This is estimated by averaging the smoothed velocity components between about 750 m and the bottom of the cast (a maximum of about 1500 m) on the assumption that deep slope currents are small. The deeper profiles often show a substantial region of near-constant speed and direction near the bottom of the profile. Directly measured deep currents over the slope (Hamilton 1990) are observed to be weak (<15 cm s^{-1}). The removed velocities often have magnitudes of 10–12 cm s^{-1}, which are about twice the maximum values reported by Sandford et al. (1987) and Glenn et al. (1990) using similar procedures. However, the near-surface velocities of the smoothed and corrected AXCP profiles agree very well with velocities estimated from drifters and current meters.

c. Current meter velocities

The shelf-break current meter data were obtained from the LATEX A program and filtered consecutively with 3- and 40-h low-pass Lanzcos kernels. The resulting 40-HLP records are decimated to 6-h intervals and rotated so that the v component is aligned with the general trend of the isobaths at the mooring site. This is indicated by the notation Rθ, where θ is the direction (deg True) of the v component, after the instrument ID which consists of the mooring number appended with T, M, or B (for top, middle, and bottom). For example, the 12-m instrument on mooring 4 is identified by “04T R25.” The data are presented as 40-HLP time series or daily averaged vectors obtained from the 40-HLP velocities.

d. Hydrographic fields

All hydrographic data has been gridded using the statistical interpolation method given by Pedder (1993), which is an iterative method similar to the Barnes (1964) two-pass scheme and its successors. In the majority of interpolations the influence scale, estimated as a mean separation of data points over the grid, used by the Gaussian influence function, is taken to be 40 km. The method is iterated to convergence (usually between 16 and 40 iterations) so that the differences between interpolated and observed fields at the data points are minimized. More details of the method can be found in Pedder (1993).

To calculate dynamic height fields, salinities have to be estimated from the XBT temperature profiles. The method is as follows: the differences between depths calculated from travel time for the XBTs and pressure for the CTDs are corrected for the T7 XBTs using the formulas given by Singer (1990). The salinities for each temperature are estimated by taking the five nearest CTD profiles from the same survey or different surveys of similar features. The salinities are weighted by $1/(R + 1)$, where R is the distance in kilometers from the XBT to the CTD station. In the first two years of the LATEX C

program, the aircraft surveys were usually preceded or followed by one of the GulfCet cruises, which included CTD casts (Table 2). In the third year, the GulfCet cruises, from the same time of year as the XBT survey in question, were still the primary source of CTD data, sometimes supplemented by the AXCTD data from flight F21SLOPE and older CTD casts from specific features such as LC eddies. For surface dynamic height anomalies, using estimated salinities, relative to 780 dbar (the deepest depth of stretched XBT profiles), the accuracies are approximately ~2 and ~5 dyn cm for using GulfCet CTD data from the same or adjacent months in the same or different years, respectively (Table 2). The dynamic height anomaly calculations for the slope region employ the method given by Csanady (1979) for integrating the bottom density profile across the isobaths. Both the GulfCet and LATEX C surveys used transects that were perpendicular to the general trend of the slope isobaths. Only stations with bottom depths less than 780 m on the upper slope require the integration of bottom densities from south to north along the transects (Csanady 1979). The method is considered accurate if the bottom σ_t isolines are approximately parallel to the isobaths so that the integration along the transect is independent of position. This is a reasonable assumption on the upper slope.

After the dynamic height anomaly is gridded, geostrophic velocity and relative vorticity are calculated using straightforward finite difference formulas. The geostrophic velocities are slightly smoothed with one pass of a Shapiro (1975) filter that suppresses any 2Δ noise in the fields where Δ is the grid spacing of order 10 km.

3. Results

The smoothed orbits of drifters in eddies U, V, W, and Y are given in Fig. 1. Brief descriptions of the life histories of these eddies, as far as they can be inferred from the data, follow below. Reasonable speculation on the sequence of events is sometimes needed where data is incomplete or missing.

Eddy U was initially a large (diameter ~300 km), vigorous Loop Current eddy that formed in the early summer of 1992. In Fig. 1a, drifter 02447 made one circuit of the eddy in late August 1992 and then entered a smaller anticyclonic eddy, located to the northwest over the base of the slope at about 92.5°W. This smaller anticyclone, named eddy V, appears from *ERS-1* altimetry to have been shed from eddy U during August and September 1992 (see Fig. 7 in Biggs et al. 1996). Eastward flow, along the periphery of the still-combined eddies U and V, was observed between 27.5° and 26.5°N at hydrographic stations over the lower slope in mid-August 1992 (F02SLOPE and GulfCet02 surveys). A separation (at station 11, Fig. 1a) between eddies U and V was evident in an AXBT transect (F04LEDDY) on 11 October 1992 and was confirmed by a Ship-of-Opportunity Program (SOOP) hydrographic transect for 28–31 October 1992, when eddy U was seeded with drifter 02449. Thus, between August and November 1992, eddy U remained in much the same position at about 91°W (Fig. 1a). Eddy U subsequently moved to the southwest as tracked by drifter 02449, eventually merging with a remnant of eddy T in the western Gulf of Mexico. Eddy T had been shed from the Loop Current about 11 months earlier than eddy U (Biggs et al. 1996).

During September to November 1992, eddy V moved westward along the base of the slope. At the end of August 1992, *ERS-1* altimetry data indicated there was a large cyclone centered about 25°N, 94.5°W (see Fig. 7d in Biggs et al. 1996). The presence of this cyclone is also indicated by the track of drifter 07493 (Fig. 1a), which skirted its periphery before moving northward over the slope under the influence of eddy V's swirl currents. This cyclone, which persisted as a more than 20 dyn cm anomaly in September and October 1992 *ERS-1* altimetry, is probably responsible for the fairly rapid westward translation of eddy V. Eddy V was surveyed a number of times between mid-November 1992 and May 1993, after its arrival at the base of the slope (2000-m isobath) in the northwestern corner of the Gulf of Mexico at about 95°W. In the latter half of December 1992, eddy V made an abrupt excursion northward onto the lower slope. Between February and April 1993, the eddy remained in the northwest corner, strongly affecting currents along the shelf break. There is some evidence from altimetry (Berger et al. 1996) that eddy V elongated along its north–south axis in April 1993 and possibly split into two. During May 1993, drifter 06938 left the shelf near 94°W and became entrained in the northern remnant of eddy V (Fig. 1b). Its track shows that this eddy was over the middle of the slope and was drifting westward toward 96°W, probably under the influence of the cyclonic circulation centered about 25°N, 95°W shown by the subsequent path of drifter 06938.

A SOOP hydrographic transect for 1–4 June 1993 and satellite AVHRR imagery from early June 1993 showed that a very large (diameter >300 km) eddy W (Walker et al. 1993) had recently detached from the LC. The ship transect found the depth of the 15°C isotherm exceeded 450 m in this eddy, and the dynamic height difference between center and periphery was +68 cm (Table 2 in Biggs et al. 1996). Drifter 02448 (Fig. 1b), initially deployed in the center of this feature, moved to the northwest and became entrained in a much smaller, fairly weak anticyclone that seems to have been shed from the massive eddy W. This small anticyclone will be called W_N. There is some evidence from altimetry (Berger et al. 1996) that a larger fragment of eddy W moved into the western Gulf in southwesterly direction at the same time when W_N was formed. After being entrained into eddy W_N, drifter 02448 showed that this eddy moved westward along the base of the slope to about 92°W. At this point, at the beginning of August 1993, the eddy and the surrounding slope were surveyed with AXBTs. The survey showed a relatively small, elongated eddy with drifter orbits similar in size to those of eddy V, but with

much less vigorous swirl velocities. The AXBT survey showed the anticyclone interacting with a cyclonic cold eddy (C1) on the lower slope at about 93°W. Drifter 06938 made a counterclockwise circuit of this cold eddy in August 1993 (Fig. 1b). The AXBT survey suggests that the interaction caused the deeper sections of eddy W_N to be forced up onto the middle slope. Immediately after the interaction, eddy W_N moved rapidly away from the slope in a south-southwest direction. This is a completely different track from that of eddy V, which remained close to the northern slope in its journey across the Gulf of Mexico. Drifter 02448 was later entrained in a large anticyclone situated in deep water at about 24°N, 93.5°W. This circulation was probably the major fragment of the original eddy W, which the altimetry indicated moved fairly rapidly westward while the northern portion (W_N) remained stalled on the lower northern slope. Therefore, it appears that drifter 02448 and eddy W_N (Fig. 1b) were reentrained into eddy W in September 1993 and tracked its interaction with the Mexican slope until January 1994. Throughout this five-month period, eddy W moved slowly northward along the base of the Mexican slope with little evidence of any decrease in size or vigor of its circulation.

Eddy X was shed from the Loop Current in the fall of 1993. Unfortunately, it was not successfully seeded with a drifter nor transited by a SOOP cruise; thus, the details of its life history can be inferred only from SST and SSH remote sensing data. It will not be discussed further in this paper.

Eddy Y detached from the Loop Current during the summer of 1994. It was seeded with two drifters, 12376 and 12377, in September 1994 and was surveyed once in October and twice in November of that same year. It was also surveyed by SOOP cruises in October and again in November 1994 (see Table 2 in Biggs et al. 1996). The eddy was of moderate size and was tracked as it moved west-southwestward, seaward of the 2000-m isobath, until it reached about 94°W in February 1995 (Fig. 1c). At this point, the drifters moved out of the eddy and indicate interactions with a large slope cyclone (C2) to the north, and an anticyclone (possibly a remnant of eddy X) to the west, against the Mexican slope (Fig. 1c). Because two drifters were simultaneously tracking eddy Y for about four months, they provide an opportunity to compare the results of the ellipse model for the two tracks and determine if the type of orbit distortions discussed by Glenn and Ebbesmyer (1993) occur for this eddy. The LATEX hydrographic surveys ended in November 1994; therefore only the early stage of eddy Y's life history, while it was over the deep water of the central Gulf, was surveyed.

a. Kinematic analyses

The ellipse parameters for eddies V (buoys 02447 and 02451, drogued at 6 and 50 m, respectively), U (buoy 02449, drogued at 100 m), W (buoy 02448, drogued at 50 m), and Y (buoys 12376 and 12377, both drogued at 100 m) are given in Figs. 2–5, respectively. Eddies U and Y follow paths and have similar characteristics to other previously studied Gulf of Mexico anticyclones (Kirwan et al. 1984a; Lewis et al. 1989; Glenn and Ebbesmyer 1993). The analyses show a general increase in rotational period over time, small divergence *D*, and relatively unsteady translation speeds characterized by periods of rapid translation followed by relative stalls, clockwise rotation of ellipse axes that slow with time and often become stationary in the far western part of the Gulf, and swirl velocities that decay quite slowly. Superimposed on these trends, some of the records have long period (25–30 day) oscillations of the parameters [e.g., eddy V after 15 December 1992 (Fig. 2) and eddy U after February 1993 (Fig. 3)]. An example of the stalls and sprints in the eddy center positions is given in the first half of the translation velocity records for eddy U (Fig. 3), where there is a relatively slow drift to the west at ~5 cm s^{-1} followed by a "sprint" (speeds >10 cm s^{-1}) to the southwest in December 1992. A more detailed analysis, given below, of the stalls and sprints of eddy Y and the accompanying departures from solid body rotation is possible because of the two concurrent drifter tracks.

Another common feature of mature eddies is their almost constant ζ. Both U (after February 1993) and W (after October 1993) show changes in rotational period being compensated by changes in eccentricity [see (3)]. Total vorticity, $f + \zeta$, tends to increase between the central and western Gulf. For conservation of total vorticity, the magnitude of ζ would need to decrease because of the southwesterly paths. Only about half the observed magnitude decrease is accounted for by the change in *f*.

Eddy V (Fig. 2) has many similar characteristics to the other eddies except that its center track is much farther north than previously observed. After moving rapidly due west along the base of the slope and stalling in the northwest corner from about 5 November to 15 December 1992, the center was displaced up onto the slope and some large perturbations in center position and orbital parameters follow. Some aspects of these perturbations were caught by surveys.

The subsidiary anticyclone, W_N, tracked by the first part of the buoy 02448 path, shows the characteristics of decay (Fig. 4). Relative, and therefore, total vorticity decreased and, if potential vorticity is conserved, the depth of the isotherms would be expected to shoal. The 4 August 1993 survey indicate a weak anticyclone with the depths of the 15° and 8°C isotherms at only 300 and 600 m, respectively. This compares to 375 and 725 m for the similar sized but vigorous eddy V at a nearby position on the slope in October 1992. As the mean radii of the orbits become smaller in July and August, the rotational period becomes shorter. This shows that the eddy is not in solid body rotation; otherwise, the center would not be

rotating faster than the edges and the period would be approximately constant.

b. Orbit distortions

The center paths of the orbits of 12376 and 12377 in eddy Y show two regions of substantial discrepancies. The first is from about 1 to 15 November when both eddy centers accelerate to the northwest and then abruptly to the south, returning to the general southwest trend of the eddy center path. Even though the paths are similar, the phasing of the changes in translation velocities are different. This event will be examined in more detail below. The second event occurs between 15 December and 10 January. In this event, the center positions of 12376 have large deviations both to the south and north of the westerly trending path of 12377. However, this period contains the last two very large highly elliptical orbits 12376 before it is expelled from the eddy (Fig. 1c). These orbits have substantially longer rotational periods than the smaller orbit of 12377 (Fig. 5); therefore, 12376 is probably orbiting outside the core of Y and being influenced by external circulations that could distort the orbit fits for this buoy. Illustrations of the orbits for 21 December and 5 January are given in Figs. 6e and 6f, respectively.

Selected orbits for both buoys are given in Fig. 6. On 6 November the center of 12377, the outer orbit, has moved past the center of the inner orbit. By 11 November the positions of the centers have reversed, with 12377 lagging 12376. The centers become approximately coincident on about 21 November. The alignments of the inner and outer orbit centers on 6 and 11 November are approximately in the direction of subsequent propagation to the northwest and south, respectively. However, these directions differ from the southwesterly direction that would be predicted by topographic Rossby wave dispersion, which dominates over planetary Rossby wave dispersion on the lower slope following the arguments of Smith (1986) and Glenn and Ebbesmeyer (1993). A more likely explanation of the distortion is the interaction of Y with a cyclone situated on the lower slope at about 93°W, shown in the 8°C isotherm depth maps in Figs. 6a and 6c. The initial northward movement of the eddy between 6 and 11 November is probably a result of the self-advective tendency by the strong northward flows between cyclone and anticyclone.

The abrupt move of Y to the south after 11 November could be a result of the mutual rotation of the cyclone–anticyclone pair in the direction of the stronger anticyclonic vortex. The cyclone is propagating northward onto the slope at roughly 5 km day^{-1}, as can be seen by comparing Figs. 6a and 6c. This movement is much slower than the orbital velocities of outer part of Y and the speed of rotation of the ellipse axes. This may indicate that the shallow depths of the slope are constraining the motion of cyclone around Y and to compensate Y moves back into deeper water and resumes solid body rotation as can be seen in Fig. 6d for 1 December. There is little evidence of any substantial change in size or change in rotational periods, and therefore vorticity (Fig. 5), during this event. Thus, eddy Y's encounter with the cyclone seems to have caused geometric distortion of orbital circulation and a perturbation in the path of the eddy center but otherwise left the eddy unscathed.

A similar conclusion can be drawn from the encounter of W_N with its cyclone (C1) in August 1993. The hydrographic survey showed the eddy being perturbed by the slope cyclone to the west. The track of drifter 06938 shows the position of the cyclone, and the dynamic height and geostrophic velocity fields (Fig. 7) suggest that C1 circulation was connected to the large elliptical cyclone shown by the July track of 06938 (Fig. 1b). Both cyclone and anticyclone are highly elliptical with eccentricities of 3.4 and 2.1, respectively. Vorticity from the drifter orbits (the cyclone rotational period is 11 days) have similar magnitudes, and this is also apparent from the surface vorticity map (Fig. 7c). The cyclone has a strong presence, and the effect is to split the anticyclone's vorticity into two parts. The anticyclonic patch in the middle of the slope almost exactly complements the cyclone's vorticity. The deep temperature field shows a similar pattern with the deep warm anomaly of W_N advected northward around the strong cold anomaly of the cyclone (not shown). In the surface layer, the cyclone is barely observed, and the warm surface water of W_N has a more conventional elliptical shape (not shown). The geostrophic velocity field shows a speed distribution that does not increase linearly from the center of W_N and explains why the buoy orbits faster with smaller mean radii (Fig. 7b).

The interaction of W_N with the cyclone seems to cause the anticyclone to begin to split into two. One consequence is the generation of a strong northward jet between the two eddies, which bifurcates just south of the shelf break producing onshore flow nearing mooring 11 and strong eastward flows east of 92°W, agreeing with the velocities observed at moorings 12 and 13 (Figs. 7a and 7b). Comparing the dynamic height anomalies at 0 and 400 dbar (Figs. 7a and 7d) shows that one effect of the northward flow is to move the deep positive and negative anomalies farther north and closer together than indicated by their surface expressions and the track of the surface drifts 06938 around the cyclone.

The final example of an eddy moving up on the slope with accompanying distortions in the circulation is the abrupt movement of eddy V onto the midslope followed by a return to the base of the slope in December 1992 and January 1993. In this case, however, there is no obvious cause such as another adjacent vigorous eddy captured either by drifters or surveys. Following the movement onto the slope and the period of rapidly converging orbits at the end of December, the

hydrography (Fig. 8a) shows the buoy track was within the 130 dyn cm contour, but AXCP averaged velocities indicate that solid body rotation extended out to about the 110 dyn cm contour in the northwest corner. The strongest currents, both observed and from geostrophy (Fig. 8b), were on the northern and northwestern edges, implying that the eddy would move southward, which it subsequently did toward the end of January.

Figure 8c shows the tracks of three drifters orbiting eddy V at the end of January. Two (02451 and 07835), drogued at 50 m, followed parallel tracks, and the analysis of the inner complete orbit placed the center on the 2000-m isobath with the major axis directed toward the northwest. The near-surface drifter (02447) analysis for 21 January 1993, however, placed its ellipse center about 30 km north of the 2000-m isobath with the major axis directed northward. This center from surface drifter was also translating southeastward, whereas the deeper center was almost stationary. All the other parameters (Fig. 2) are reasonably consistent with each other for the two analyzed drifters. The rms errors in the orbit fits are <10 km and, because the inner and outer orbits of 02451 and 07835 are similar though 07835 is clearly in the outer cyclonic shear zone of the eddy, topographic Rossby wave dispersion does not account for the center differences because it would also be apparent in these orbits and the ellipse axes would be aligned. The inference is that the deeper layers of the eddy return to an equilibrium position after the eddy was forced northward onto the slope, more rapidly than the surface layers, causing the vertical axis of rotation to tilt.

By the time of the next hydrographic survey (Gulfcet04) at the end of February (Fig. 8d), the eddy was still at the base of the slope. Rotational period, estimated from the vorticity, was about 11 days and eccentricity had increased to about 1.6 with the major axis directed north–south. There was a peripheral cyclone on the upper slope to the east, which is also hinted at in the moored currents from moorings 08 and 09 in Fig. 8c. There is also an indication from the moored currents, at 04, 47, and 05 in Fig. 8d that another cyclone was situated to the west. The R/V *Gyre* SOOP cruise 93G-03 showed that a third region of cyclonic circulation lay ESE of eddy V between 26.5° and 25.5°N along 93°W. The dynamic height field of this 100-km diameter cyclone reached a low of 88 dyn cm in the interior of this feature (Biggs et al. 1997).

4. Statistics

The statistics of the kinematic parameters are summarized in Table 3 in terms of means over selected portions of the paths of eddies U, V, W_N, W, and Y. There are a few general trends in these means. When an eddy approaches the Mexican slope, it seems to have a significantly longer rotational period than earlier in its life after it became separated from the Loop Current. The decrease in f, because of the southwest paths, only accounts for about half the decrease in magnitude of ζ under the assumption that $f + \zeta$ is constant, for eddies U and W. Eddies V and Y also showed increasing rotational periods with time. Second, when an anticyclone is in contact with the slope region, decay or dissipation appears to be small and occurs over timescales on the order of one month. Third, an interaction with another eddy or with slope topography seems to decrease or stop the clockwise rotation rate of the semimajor axis of the ellipse. Fourth, larger more vigorous eddies (i.e., U and Y), in the central Gulf of Mexico, tend to have longer rotational periods and slower clockwise rotation rates than their smaller cousins (i.e., V and W_N).

It is noteworthy (Table 3) that swirl velocities derived from drifters remain relatively constant. Simultaneous comparisons of drifter swirl velocities with the temperature fields show that, for a vigorous mature eddy, the drifter tracks tend to follow the 200-m contour of the 20°C isotherm. The resulting mean radii are generally about half the true radius of the region where the eddy is in approximate solid body rotation. Similar results were obtained by Glenn and Ebbesmeyer (1993) when buoy orbits and isotherm depths were compared. When the eddy begins to slow its rotation rate, the drifter tends to move to a larger radius, closer to the edge, thereby maintaining swirl velocity magnitudes. Thus, the drifter-derived swirl velocities alone may not be a good indication of the vigor of an anticyclone.

A comparison of average relative vorticity ζ calculated from dynamic height and from buoy orbit parameters by (3) is given in Table 4 for hydrographic surveys listed in Table 2 and marked by event lines in Figs. 2–5. Calculations of ζ from dynamic height are inherently noisy, and the results are dependent on the resolution of the stations, how much of the eddy is mapped, and the influence scale of the Gaussian filter used to grid the data. A conservative estimate of the accuracy for a relatively low resolution survey (e.g., Gulfcet04, Fig. 8d) is $\pm 5 \times 10^{-6}$ s^{-1}. For the calculations in Table 4, ζ is averaged for the region inside the dynamic height contour that best coincides with the buoy orbit and for the region of the eddy where ζ is negative (or positive for W_N's cyclone). The best database is for eddy V, and the maximum dynamic height anomaly and relative vorticity have quite a bit of variability over the five cruises. Therefore, there is some support for the notion that eddy V was affected by exchanges with adjacent eddies such as U and the northern remnants of T. The means of all the realizations are reasonably consistent with the buoy orbit derived ζ, being about 150% of the equivalent ζ, derived from hydrography, which is only a little greater than the magnitude of the negative ζ region. The orbit calculations assume solid body rotation and, thus, homogenous ζ inside the orbit. The differences with the hydrography indicate deviations from this assumption for the surface geostrophic velocity fields of an average anticyclone. The largest discrepancies between the three measures of ζ was for the August 1994 survey of W_N, which was clearly not in solid body

rotation as discussed above.

5. Ensemble statistics

The previous section summarizes the statistics of the individual Loop Current eddies studies during the LATEX program. This section calculates mean Lagrangian statistics for eddies tracked with drifters for more than one month between 1985 and 1995. The drifter paths prior to LATEX were obtained by the previous Gulf of Mexico Physical Oceanography Program, and their kinematic analyses are given in SAIC (1988, 1989), Lewis et al. (1989), and Biggs et al. (1996). For this analysis, these paths were smoothed and parameters calculated using the least square ellipse model of Glenn et al. (1990), exactly the same as for the LATEX drifters discussed above. Table 5 gives the eddy names and the drifters that were analyzed. Figure 9 shows the paths of the centers of these eddies derived from the ellipse model calculations.

The ensemble of eddy paths in Fig. 9 has a predominantly southwesterly trend and occupies a broad area of 2°–3° latitude in width in the center of the deep basin. In this context, the path of eddy V appears to be anomalous in that it moves from east to west (Fig. 1a) and is closer to the slope than any other observed eddy. There are substantial deviations from the southwesterly trend near the Mexican slope. Therefore, in the statistics, the paths have been divided into portions that are east and west of 94°W (Table 5) so that eddies propagating through the deep basin are separated from those eddies being influenced by the topography of the Mexican slope.

Following Davis (1985), the Lagrangian auto- and cross-correlations of the u and v components of the center translation velocities are calculated for each path (or partial path) in Fig. 9 that is east or west of 94°W and then ensemble averaged. The results are given in Fig. 10. In the deep basin, the Lagrangian autocorrelation timescale is about 5 days for both components. This is about half the mean eddy period. West of 94°W, the u and v component timescales are about 13 and 7–8 days, respectively, which are on the order of the eddy period. Autocorrelation timescales for the smoothed drifter velocities are about half the eddy period, as would be expected for strongly circular motions (not shown). The eddy center velocity ensemble mean cross-correlations are relatively weak in the basin, but significant near the slope. For the latter, v lags behind u by 7 days, and the symmetrical shape indicates a periodicity on the order of 20 days. Examination of the paths in Fig. 9 shows many portions with anticyclonic curvature and periodicities on the order of 20–30 days in all parts of the Gulf of Mexico. This periodicity was also noted in the individual analyses of eddies V, U + T, and W. Thus, Lagrangian timescales are relatively short compared to the ~ 100-day path length, but increase toward the slope and become less isotropic with the east–west (u) timescale, becoming longer as the east–west locations become more stationary adjacent to the slope.

Vukovich and Crissman (1986) analyzed eddy paths from imagery and indicated that northward movement is characteristic of eddies colliding with the slope around 23°–24°N. This is the case for several eddies tracked by drifters, including eddy W (Fig. 1b) and the eddy tracked by Kirwan et al. (1984a). In this limited sample of seven drifter-tracked eddies, however, the ensemble mean, northward translation velocity component (Table 6) is not significantly different from zero, and, therefore, there seems to be no preferred direction of propagation along the slope after the eddies collide with the western boundary. Possible explanations of this difference in path statistics between the two types of data are the limited sample size, and also there may be biases in the imagery database because of relatively high degree cloud cover and low thermal contrast in the Bay of Campeche that makes eddies difficult to track in this region.

In Table 6, mean radii and swirl velocities decrease between east and west, but the period only increases by 0.6 days. This is less than observed for individual eddies, such as U (Fig. 3), and may be the result of using a different set of eddy paths in each of the regions. However, these three parameters together indicate a weakening of the eddy circulation in the west.

Mean ellipse eccentricities are close to the expected β Rossby number (1.5) for eddy shedding by the Loop Current (Hurlburt and Thompson 1982). Relative vorticity is basically constant in the two regions, However, mean latitudes for the paths east and west of 94°W differ by about 1.5° and thus, mean total vorticity decrease by -1.7×10^{-6} s^{-1} between east and west. These statistics indicate a relatively slow decay of circulation as eddies propagate across the western Gulf and interact with the western slope. This is consistent with Elliott's (1982) estimate of O(1 yr) decay timescale for western gulf eddies based on hydrographic survey data.

6. Summary

The kinematics and paths of Loop Current anticyclones in the western Gulf of Mexico have been studied using the Glenn et al. (1990) feature model applied to Lagrangian drifter tracks. Buoy data from 1992 to 1994 obtained during the LATEX program were used to characterize the unusual behavior of eddies V and W_N, and eddies V, W, and Y. The latter had many similarities to eddy paths previously analyzed by Kirwan et al. (1984b), Lewis et al. (1989), and Glenn and Ebbesmyer, (1993) among others.

A few of the eddies (V, W_N, and Y) were surveyed by ship and aircraft at different stages of their lives. Maps of dynamic height anomaly and relative vorticity were compared with buoy orbit analyses where appropriate. Eddy V was apparently shed from the much larger U that in September 1992 moved rapidly westward along the base of the slope and stalled in the northwest corner of the Gulf. It made an excursion into shallower water in January 1993 that involved distortion of the orbits of different drifters drogued at the surface and 50 m, which caused the central axis of rotation to tilt. The path of V was much closer to the slope than other "northern path" eddies such as fast eddy (B) (Lewis et al. 1989) and Y, and its behavior was also different than B's when it reached the western boundary in that a companion cyclone was not generated in the manner shown by Lewis et al. (1989) and the model of Smith (1986).

Eddy W_N was also a subsidiary anticyclone of the much larger eddy W, and W_N also initially propagated westward along the base of the slope to 91.5°W where it strongly interacted with a cyclone on the lower slope. Unlike V, W_N had a fairly weak circulation that decayed quite rapidly over its 4-month lifetime and it is doubtful that its circulation was ever in solid body rotation. A hydrographic survey showed strong distortions of the anticyclone's vorticity and dynamic height fields caused by the encounter with the slope cyclone.

For eddy Y, which tracked quite steadily southwestward, parallel to the isobath trends of the northern slope in the second half of 1994, an encounter with a lower slope cyclone was documented. This event caused a northward perturbation of the center path and displacements of the inner and outer orbits of the two buoys in the eddy. The offsetting of the center of the orbits, and the departure from solid body rotation, has been observed before and attributed to topographic and planetary Rossby wave dispersion by Glenn and Ebbesmyer (1993). In this event, the direction of the displacements was not consistent with topographic Rossby wave dispersion and was more likely a result of the interaction with the cyclone.

Another characteristic that was observed for eddies U, V, and W as they approached the western slope was the presence of 20–30 day oscillations of the ellipse parameters. Ensemble statistics of ten historical eddies also showed similar period anticyclonic perturbations of the center paths of the orbits obtained from the feature model. It may be significant that the spectra of deep currents obtained from moored arrays also show prominent 20–30 day period peaks that have been attributed to topographic Rossby waves (Hamilton 1990).

The ensemble statistics also showed that there were no preferred areas of the deep basin for eddies as the paths were fairly evenly distributed by latitude. Therefore, a distinction between northern and southern eddy paths may be artificial. There was also no bias in the north–south direction that eddies take after encountering the western slope. Vukovich and Crissman (1986), using imagery to track eddies determined that eddies that impinged on the slope around 23°–24°N (the majority) tended to migrate northward along the slope. Lagrangian timescales calculated from translation velocities of the eddies were about 5 days in the basin and 13 days against the slope. Based on rotational period, relative vorticity and mean radius, the decay of eddies between the main basin and the western slope is quite small.

Acknowledgments

The data used for this paper were obtained by the LATEX C, LATEX A, GulfCet, and Ship of Opportunity Program projects funded by Minerals Management Service (MMS) on Contracts 14-35-0001-30633 to Science Applications International Corporation, Raleigh, North Carolina; and 14-35-0001-30509, 14-35-0001-30619, and 14-35-0001-30501 to Texas A&M University. P. Hamilton, G. Fargion, and D. Biggs were supported by the LATEX C, GulfCet, and SOOP projects, respectively. Thanks are due to Alexis Lugo-Fernandez and Murray Brown, the project officers, and Tom Berger, the program manager for LATEX C, for help and encouragement during the preparation of this paper. Matthew Howard of Texas A&M University provided the shelf-break LATEX A current meter data for this study. The AXBT surveys were performed by Aero Marine Surveys under the direction of Tim Flynn and Tom Berger.

REFERENCES

Barnes, S., 1964: A technique for maximizing details in numerical map analysis. *J. Appl. Meteor.*, **3,** 395–409.. Find this article online

Berger, T. J., P. Hamilton, J. J. Singer, R. R. Leben, G. H. Born, and C. A. Fox, 1996: Louisiana/Texas Shelf physical oceanography program: Eddy circulation study, final synthesis report. Vol. I. Tech. Report, OCS Study, MMS 96-0051, U.S. Department of the Interior, Minerals Management Service, Gulf of Mexico OCS Region, New Orleans, LA, 324 pp..

Biggs, D. C., G. Fargion, P. Hamilton, and R. Leben, 1996: Cleavage of a Gulf of Mexico Loop Current eddy by a deep-water cyclone. *J. Geophys. Res.*, **101,** 20 629–20 641..

— ,R. Zimmerman, R. Gasca, E. Suarez, I. Castellanos, and R. Leben, 1997: Note on plankton and cold-core rings in the Gulf of Mexico.

Fish. Bull., **95,** 369–375..

Brooks, D. A., and R. V. Legeckis, 1982: A ship and satellite view of hydrographic features in the western Gulf of Mexico. *J. Geophys. Res.*, **87,** 4195–4206..

Csanady, G. T., 1979: The pressure field along the western margin of the North Atlantic. *J. Geophys. Res.*, **84,** 4905–4913..

Davis, R. E., 1985: Drifter observations of coastal surface currents during CODE: The statistical and dynamical views. *J. Geophys. Res.*, **90,** 4756–4772..

Elliot, B. A., 1982: Anticyclonic rings in the Gulf of Mexico. *J. Phys. Oceanogr.*, **12,** 1292–1309.. Find this article online

Glenn, S. M., and C. C. Ebbesmeyer, 1993: Drifting buoy observations of a Loop Current anticyclonic eddy. *J. Geophys. Res.*, **98,** 20 105–20 119..

— ,G. Z. Forristall, P. Cornillon, and G. Milkowski, 1990: Observations of Gulf Stream ring 83-E and their interpretation using feature models. *J. Geophys. Res.*, **95,** 13 043–13 064..

Hamilton, P., 1990: Deep currents in the Gulf of Mexico. *J. Phys. Oceanogr.*, **20,** 1087–1104.. Find this article online

— ,1992: Lower continental slope cyclonic eddies in the central Gulf of Mexico. *J. Geophys. Res.*, **97,** 2185–2200..

Hurlburt, H. E., and J. D. Thompson, 1982: The dynamics of the Loop Current and shed eddies in a numerical model of the Gulf of Mexico. *Hydrodynamics of Semi-Enclosed Seas*, J. C. J. Nihoul, Ed., Elsevier, 243–298..

Johnson, D. R., J. D. Thompson, and J. D. Hawkins, 1992: Circulation in the Gulf of Mexico from GEOSAT Altimetry during 1985–1986. *J. Geophys. Res.*, **97,** 2201–2214..

Kirwan, A. D., Jr., W. J. Merrell Jr., J. K. Lewis, and R. E. Whitaker, 1984a: Lagrangian observations of an anti-cyclonic ring in the western Gulf of Mexico. *J. Geophys. Res.*, **89,** 3417–3424..

— ,— ,— ,— ,and R. Legeckis, 1984b: A model for the analysis of drifter data with an application to a warm core ring in the Gulf of Mexico. *J. Geophys. Res.*, **89,** 3425–3438..

— ,J. K. Lewis, A. W. Indest, P. Reinersman, and I. Quintero, 1988:Observed and simulated kinematic properties of Loop Current rings. *J. Geophys. Res.*, **93,** 1189–1198..

Leben, R. R., and G. H. Born, 1993: Tracking Loop Current eddies with satellite altimetry. *Adv. Space Res.*, **13,** 325–333..

Lewis, J. K., A. D. Kirwan Jr., and G. Z. Forristall, 1989: Evolution of a warm-core ring in the Gulf of Mexico: Lagrangian observations. *J. Geophys. Res.*, **94,** 8163–8178..

Merrell, W. J., and J. M. Morrison, 1981: On the circulation of the western Gulf of Mexico with observations from April 1978. *J. Geophys. Res.*, **86,** 4181–4185..

Nof, D., 1988: The fusion of isolated nonlinear eddies. *J. Phys. Oceanogr.*, **18,** 887–905.. Find this article online

Pedder, M. A., 1993: Interpolation and filtering of spatial observations using successive corrections and Gaussian filters. *Mon. Wea. Rev.*, **121,** 2889–2902.. Find this article online

SAIC, 1988: Gulf of Mexico physical oceanography program, final report: year 3. Vol. II. Tech. Report, MMS Contract 14-12-0001-29158, OCS Rep. MMS 88-0046, U.S. Department of the Interior, Minerals Management Service, Gulf of Mexico OCS Region, New Orleans, LA, 241 pp. [Available from Public Information Office (MS 5034), 1201 Elmwood Park Blvd., New Orleans, LA 70123.].

— ,1989: Gulf of Mexico physical oceanography program, final report: year 5. Vol. II. Tech. Report, MMS Contract 14-12-0001-29158, OCS Rep./MMS 89-0068, U.S. Department of the Interior, Minerals Management Service, Gulf of Mexico OCS Region, New Orleans, LA, 333 pp. [Available from Public Information Office (MS 5034), 1201 Elmwood Park Blvd., New Orleans, LA 70123.].

Sanford, T. B., P. G. Black, J. R. Haustein, J. W. Feeney, G. Z. Forristall, and J. F. Price, 1987: Ocean response to a hurricane. Part I: Observations. *J. Phys. Oceanogr.*, **17,** 2065–2083.. Find this article online

Shapiro, R., 1975: Linear filtering. *Math. Comput.*, **29,** 1094–1097..

Singer, J. J., 1990: On the error observed in electronically digitized T-7 XBT data. *J. Atmos. Oceanic Technol.*, **7,** 603–611..

Smith, D. C., 1986: A numerical study of Loop Current eddy interaction with topography in the western Gulf of Mexico. *J. Phys. Oceanogr.*, **16,** 1260–1272.. Find this article online

Vidal, V. M. V., F. V. Vidal, and J. M. Pérez-Molero, 1992: Collision of a Loop Current anticyclonic ring against the continental slope of the western Gulf of Mexico. *J. Geophys. Res.*, **97,** 2155–2172..

— ,— ,A. F. Hernandez, E. Meza, and J. M Pérez-Molero, 1994:Baroclinic flow, transports, and kinematic properties of a cyclonic-anticyclonic-cyclone ring triad in the Gulf of Mexico. *J. Geophys. Res.*, **99,** 7571–7597..

Vukovich, F. M., and B. W. Crissman, 1986: Aspects of warm rings in the Gulf of Mexico. *J. Geophys. Res.*, **91,** 2645–2660..

Walker, N. D., O. K. Huh, and L. J. Rouse Jr., 1993: Recent loop eddy separation in the Gulf of Mexico. *Eos., Trans. Amer. Geophys. Union*, **74,** 30..

Tables

Table 1. Gulf of Mexico LATEX drifters.

Drifter ID	Deployment date	Stop date	Drogue type	Drogue depth (m)	Eddies
7493*	20 Aug 92	18 Sep 92	1 × 3	3	C6
2447	10 Aug 92	1 Feb 93	1 × 3	6	U, V
2449	30 Oct 92	17 Apr 93	1 × 7	100	U
2451	9 Jan 93	5 Feb 93	1 × 7	50	V
7835	9 Jan 93	5 Jun 93	1 × 7	50	V
6938	29 Apr 93	24 Sep 93	1 × 3	6	V, C1
2448	5 Jun 93	18 Jan 94	1 × 7	50	W_N, W
12376	17 Sep 94	26 Feb 95	1 × 7	100	Y
12377	12 Oct 94	30 Apr 95	1 × 7	100	Y

* NDBC experimental spar buoy.

Click on thumbnail for full-sized image.

Table 2. Gulf of Mexico northern slope hydrographic surveys.

Cruise ID	Dates	AXBT	AXCP	XBT	CTD
Gulfcet02	11–23 Aug 92	—	—	78	44
F04LEDDY	11 Oct 92	16	—	—	—
Gulfcet03	10–21 Nov 92	—	—	76	38
F05LEDDY	19 Dec 92	16	—	—	—
F06SPECI	4–6 Jan 93	42	6	—	—
Gulfcet04	12–24 Feb 93	—	—	82	43
F08SLOPE	12–16 May 93	36	—	—	—
F09SEDDY	18–19 May 93	13	4	—	—
Gulfcet05	24 May–30 Jun 93	—	—	71	42
F10SLOPE	3–4 Aug 93	35	—	—	—
F11LEDDY	5 Aug 93	16	—	—	—
Gulfcet06	28 Aug–6 Sep 93	—	—	90	38
Gulfcet07	3–14 Dec 93	—	—	73	32
F18LEDDY	15 Oct 94	3	13	—	—
F19SEDDY	16–17 Oct 94	46	—	—	—
F20SLOPE	4–8 Nov 94	68	2	—	—
F21SQUIRT	11–16 Nov 94	71	18	—	6*

* AXCTD.

Click on thumbnail for full-sized image.

Table 3. Summary statistics of ellipse model parameters.

			Mean				Mean clockwise rotation rate of major axis (deg day^{-1})	
Eddy	Drifter	Dates	Period (days)	Translation speed (cm s^{-1})	Swirl speed (cm s^{-1})	Radius (km)		Comments
V	02447	20 Sep–11 Nov 92	7.3 ± 0.6	6.8 ± 2.7	55 ± 11	35 ± 9	8	Westward translation to 85°W
V	02447	11 Nov 92–21 Jan 93	8.3 ± 1.0	4.4 ± 2.7	48 ± 7	35 ± 8	4	Interaction with slope
V	08038	12 May–3 Jun 93	9.4 ± 1.1	6.7 ± 2.8	49 ± 8	42 ± 5	0	Final stages of decay on upper slope
U	02449	6 Nov 92–2 Jan 93	10.3 ± 1.2	5.9 ± 3.4	34 ± 7	48 ± 6	4	Southwestward translation across central Gulf of Mexico
U + ?	02449	19 Jan–30 Mar 93	12.7 ± 1.5	5.4 ± 2.7	28 ± 8	50 ± 17	2.5	Approach to Mexican slope
W_N	02448	7 Jul–8 Aug 93	8.2 ± 1.2	5.7 ± 2.0	17 ± 9	20 ± 13	4.5	Interaction with slope cold eddy
W_N	02448	8 Aug–2 Sep 93	6.3 ± 0.5	8.6 ± 2.6	36 ± 9	31 ± 9	0	SSW translation into western Gulf of Mexico
W	02448	19 Sep–15 Oct 93	13.8 ± 1.7	7.3 ± 3.0	43 ± 10	79 ± 12	2	Approach to Mexican slope
W	02448	15 Oct–5 Dec 93	13.1 ± 1.4	5.8 ± 1.9	45 ± 7	80 ± 10	2	Stalled against Mexican slope
W	02448	5 Dec 93–12 Jan 94	12.4 ± 0.9	5.6 ± 2.7	47 ± 6	80 ± 11	0	Northward migration along the Mexican slope
Y	12376	22 Sep 94–10 Jan 95	10.4 ± 2.5	5.8 ± 3.0	48 ± 9	69 ± 20	2	WSW translation 89°–93°W
Y	12377	17 Oct 94–3 Feb 95	11.3 ± 2.1	5.8 ± 3.0	47 ± 17	72 ± 22	2	WSW translation 89°–93°W

Click on thumbnail for full-sized image.

Table 4. Comparison of eddy relative vorticity from buoy orbits and dynamic height.

		Buoy orbit contour		Maximum [minimum]	Ellipse		Average relative vorticity ζ (10^{-6} s^{-1})			
Eddy [Cyclone]	Date	20°C isotherm depth (m)	Dynamic height (dyn cm)	dynamic height (dyn cm)	Area (10^3 km^2)	Eccentricity	Drifter [Eq. (5)]	Inside dyn ht. contour	$\zeta < 0$ [=0]	Cruise ID
Y	19 Nov 92	200	150	142	8.7	1.2	−20.4	−12.7	−9.2	Gulfcet03
	10 Dec 92	175	120	132	13.6	1.3	−15.1	−6.3	−6.1	F05LEDDY
	5 Jan 93	200	130	140	4.7	1.1	−15.6	−17.8	−10.4	F06SPECI
	21 Feb 93		120	126				−15.4	−11.0	Gulfcet04
	19 May 93	125	120	131	15.0	1.1	−17.1	−13.1	−12.1	F09SEDDY
W_N	7 Aug 93	175	155	181	0.8	1.1	−20.0	−18.4	−9.4	F10SLOPE
[C1]	7 Aug 93	175	160	[90]	0.8	3.4	+24.3	+10.7	+10.2	F10SLOPE
Y	15 Oct 94	200	150	189	20.6	1.1	−17.2	−11.0	−13.0	F18LEDDY
Average for anticyclones Y, W_N, and Y							−18.9	−13.5	−10.2	

Click on thumbnail for full-sized image.

Table 5. Drifters in Loop Current eddies.

E	03344	21 Nov 87–14 Feb 88	—
E	03353	—	22 Jun–11 Sep 88
F	03345	27 May–30 Nov 88	—
T	07493	26 Feb–21 Apr 92	25 Apr–30 Jun 92
U	02449	6 Nov 92–1 Feb 93	—
U + T	02449	—	19 Jan–30 Mar 93
V	02447	20 Sep–20 Oct 92	29 Oct 92–21 Jan 93
W_N	02448	20 Jan–2 Sep 93	—
W	02448	—	19 Sep 93–12 Jan 94
Y	12376	22 Sep 94–16 Jan 95	—
Total number of days		824	625

Click on thumbnail for full-sized image.

Table 6. Lagrangian mean statistics of Gulf of Mexico Loop Current eddies.

Variable	Units	Mean	Standard deviation	Principal axes*
Central Gulf of Mexico (east of 94°W)				
East translation U	cm s^{-1}	−3.76	3.93	35
North translation V	cm s^{-1}	−1.91	3.68	
Geometric mean radius	km	65.10	17.40	
Ellipse eccentricity		1.40	0.32	
Swirl velocity	cm s^{-1}	46.80	12.80	
Eddy period	days	10.20	1.60	
Relative vorticity	10^{-5} s^{-1}	−16.00	2.20	
Western Gulf of Mexico (west of 94°W)				
East translation U	cm s^{-1}	−1.96	3.81	69
North translation V	cm s^{-1}	−0.32	4.17	
Geometric mean radius	km	51.60	12.40	
Ellipse eccentricity		1.53	0.46	
Swirl velocity	cm s^{-1}	36.00	8.10	
Eddy period	days	10.80	1.90	
Relative vorticity	10^{-5} s^{-1}	−15.80	2.50	

* Principal axis direction is counterclockwise from the east.

Click on thumbnail for full-sized image.

Figures

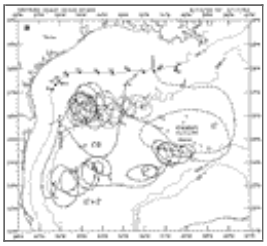

Click on thumbnail for full-sized image.

Fig. 1. Smoothed tracks for buoys (a) 02447 (dashed: eddies U and V), 02449 (solid: eddy U), and 07493 (solid: cyclone C6); (b) 02448 (solid: eddy W) and 06938 (dashed: eddy V); and (c) 12376 (solid) and 12377 (dashed: eddy Y). Arrow heads are every 5 days. In (a)

Click on thumbnail for full-sized image.

Fig. 1. (*Continued*) station positions for the F04LEDDY AXBT survey of eddies U and V are indicated with small crosses, and LATEX A numbered shelf-break moorings are marked with solid squares.

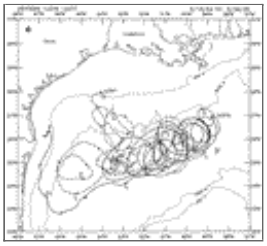

Click on thumbnail for full-sized image.

Fig. 1. (*Continued*)

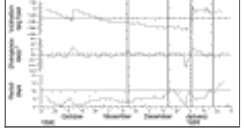

Click on thumbnail for full-sized image.

Fig. 2. Time series of ellipse parameters from model fits to the paths of buoys 02447 (solid) and 02451 (dashed) in eddy V. The parameters from the bottom are period; divergence; inclination; major, minor (dashed), and mean (heavy solid) semiaxis lengths; east (shaded) and north (dashed) translation velocity components, with translation speed (heavy solid); swirl speed; and relative vorticity. The top panel shows the 40-HLP velocity vectors from the 12-m level of mooring 49. Up is along isobath toward the east. Lines mark times of surveys and events discussed in the text.

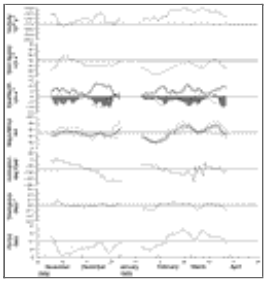

Click on thumbnail for full-sized image.

Fig. 3. Time series of ellipse parameters from model fits to the paths of buoys 02449 in eddy U. Parameters are as in Fig. 2.

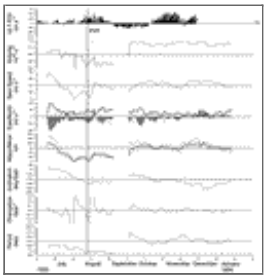

Click on thumbnail for full-sized image.

Fig. 4. Time series of ellipse parameters from model fits to the paths of buoy 02448 in eddy W. Parameters are as in Fig. 2. The top panel shows the 40-HLP velocity vectors from the 12-m level of mooring 12. Up is along isobath toward the east. Event line marks the time of the F10SLOPE survey.

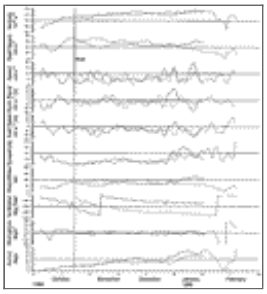

Click on thumbnail for full-sized image.

Fig. 5. Time series of ellipse parameters from the analyses of buoys 12376 (solid) and 12377 (dashed). From the bottom, the time series are period, divergence, inclination of the major axis to east, mean radius, eccentricity, east and north, translation velocity, translation speed, swirl speed, and relative vorticity. The event line marks the date of the F18LEDDY survey.

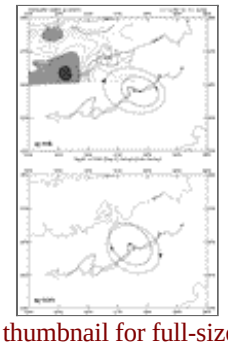

Click on thumbnail for full-sized image.

Fig. 6. Selected orbits from buoy analyses of 12376 (solid) and 12377 (dashed) for (a) 6 Nov 1994, (b) 11 Nov 1994, (c) 14 Nov 1994, (d) 1 Dec 1994, (e) 21 Dec 1994, and (f) 5 Jan 1995. (a) and (c) show the depth (m) of the 8°C temperature surface from surveys F20SLOPE and F21SQUIRT, respectively. Depths above 500 m are shaded.

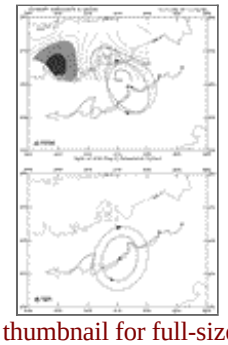

Click on thumbnail for full-sized image.

Fig. 6. (*Continued*)

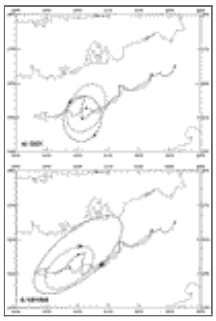

Click on thumbnail for full-sized image.

Fig. 6. (*Continued*)

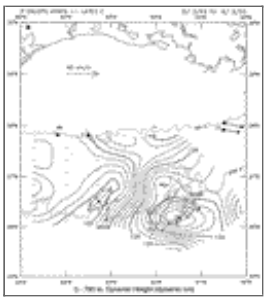

Click on thumbnail for full-sized image.

Fig. 7. Dynamic height (a), geostrophic velocity (b), and relative vorticity (c: positive values shaded) at the surface, and dynamic height at 400 dbar (d) relative to 780 dbar for the F10SLOPE and F11LEDDY surveys. Daily velocity vectors from buoys 06938 (cyclone C1) and 02448 (eddy W_N) are overlaid beginning 30 July 1993, and daily averaged

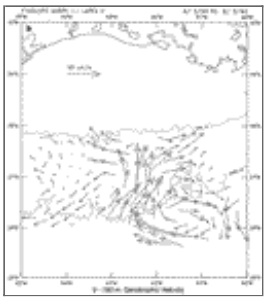

Click on thumbnail for full-sized image.

Fig. 7. (*Continued*) 40-HLP velocities from the LATEX A moorings (solid squares) from the 12-m level are shown for 4 August in (a). Ellipse axes for 2 and 12 August (buoy 02448), and 7 August (buoy 06938) are shown in (a) and (d).

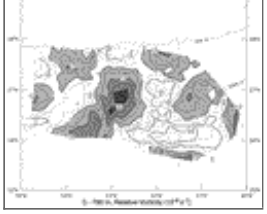

Click on thumbnail for full-sized image.

Fig. 7. (*Continued*)

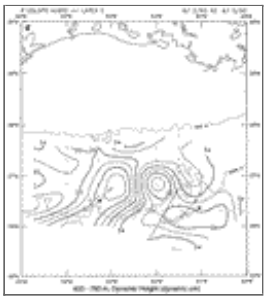

Click on thumbnail for full-sized image.

Fig. 7. (*Continued*)

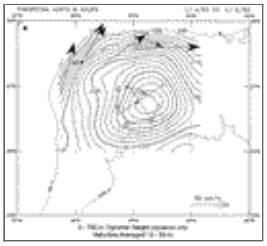

Click on thumbnail for full-sized image.

Fig. 8. Dynamic height and surface geostrophic velocity plots for survey F06SPECIAL (a,b) and dynamic height from survey Gulfcet04 (d). Average smoothed velocities from the AXCP profiles are shown as heavy dashed arrows emanating from crosses for 4–6 January (a). Daily velocity vectors from buoys 07835 (drogued at 50 m, beginning 14 January 1993), 02451 (drogued at 50 m) and 02447,

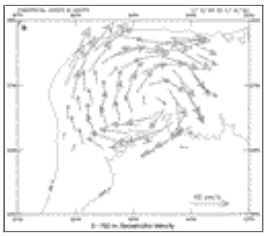

Click on thumbnail for full-sized image.

Fig. 8. (*Continued*) (drogued at 6 m; beginning 15 January) are given in (c). Daily averaged 40-HLP velocities from the LATEX A moorings (solid squares) from the 12-m (dashed) and 100-m (solid) levels are given for 25 January (c) and 21 February (d), and the ellipse axes are given for 21 January with the solid squares in the center of the eddy marking the ellipse centers 24 h earlier (c).

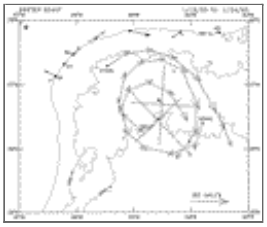

Click on thumbnail for full-sized image.

Fig. 8. (*Continued*)

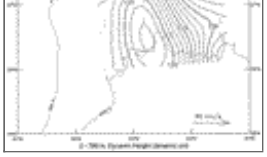

Click on thumbnail for full-sized image.

Fig. 8. (*Continued*)

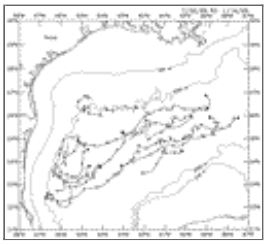

Click on thumbnail for full-sized image.

Fig. 9. Paths of center positions of the eddies given in Table 5. Arrow heads are at 10-day intervals.

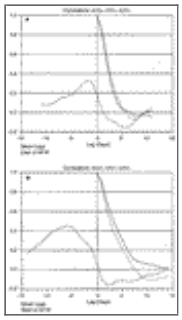

Click on thumbnail for full-sized image.

Fig. 10. Ensemble Lagrangian time-lagged correlations of east (U) and north (V) components of eddy translation velocity (‹UU› solid; ‹VV› short dashed; and ‹UV› long dashed). (a) Paths east of 94°W and (b) paths west of 94°W.

[1] The LATEX program was a major study of the Louisiana and Texas continental shelves and slopes. Parts A and C were devoted to shelf and slope physical oceanography, respectively.

* Current affiliation: Hughes/Earth Observing System Distributed Information System, Landover, Maryland.

Corresponding author address: Dr. Peter Hamilton, Science Applications International Corporation, Suite 300, 615 Oberlin Road, Raleigh, NC 27605.

E-mail: phamilton@raleigh.saic.com